

2

NRL Memorandum Report 4982

# Application of Ion Implantation Induced Damage to Electron Device Fabrication in InP

P. E. THOMPSON, S. C. BINARI, AND H. B. DIETRICH

*Solid State Devices Branch  
Electronics Technology Division*

December 15, 1982

DTIC  
ELECTRONICS  
DEC 14 1982  
S H

This work was supported by the Naval Electronic Systems Command  
and the Office of Naval Research.



NAVAL RESEARCH LABORATORY  
Washington, D.C.

Approved for public release; distribution unlimited.

82 12 14 031

A122496

FILE COPY



20 ✓ ABSTRACT (Continued)

Anomalous results were observed for H implantation in that measurements carried out by contacting the front and back of the damage layer gave resistivity values two orders of magnitude greater than those measured by contacting to adjacent points on an isolated epitaxial structure. For all other ions, the results obtained for the two geometries were in good agreement. It has been shown that a conductive layer produced by the proton bombardment of the underlying Fe-doped substrate gives rise to a low resistance shunt in the epitaxial study.

CONTENTS

INTRODUCTION ..... 1

EXPERIMENTAL PROCEDURE ..... 2

RESULTS ..... 5

    A. Vertical Isolation ..... 5

    B. Lateral Structure ..... 9

    C. Additional Studies of Proton Induced Damage ..... 9

    D. Anneal Study ..... 16

CONCLUSION ..... 21

REFERENCES ..... 22

DTIC  
COPY  
INSPECTED  
2

Accession For	
NTIS GRA&I	<input checked="" type="checkbox"/>
DTIC TAB	<input type="checkbox"/>
Unannounced	<input type="checkbox"/>
Justification	
By _____	
Distribution/	
Availability Codes	
Avail and/or	
Dist	Special
A	

APPLICATION OF ION IMPLANTATION INDUCED DAMAGE TO  
ELECTRON DEVICE FABRICATION IN InP

INTRODUCTION

In the fabrication of III-V planar structures, interdevice isolation is obtained in one of two ways. Either chemical dopants are selectively implanted into semi-insulating (SI) substrates to produce regions of active material or selected regions of active layers are compensated with implantation induced damage to produce the same effect. For the purpose of interdevice isolation, implantation-induced damage is comparable to selective implantation in GaAs and p-type InP. In these materials, resistivities of  $10^7$  ohm·cm can be obtained by proton bombardment.<sup>(1,2)</sup> However, the maximum resistivity which has been reported for proton bombardment in n-type InP is  $10^3$  ohm·cm.<sup>(2)</sup> Since this is inadequate for a variety of applications, a comprehensive study of damage induced isolation in n-type InP was initiated and the results of this work are detailed in this paper.

The study was restricted to light ions (H, He, Be, and B) because the depth of the damage layer is inversely related to the ion mass. For example, although in n-type InP Fe-implantation has been shown to produce chemical compensation with a resulting resistivity of greater than  $10^7$  ohm·cm,<sup>(3)</sup> 300 keV Fe has a projected range of only 0.15  $\mu\text{m}$  in InP.<sup>(4)</sup> For comparison, 300 keV H has a projected range of 2.6  $\mu\text{m}$ .<sup>(4)</sup> For this work, two test structures have been used to measure the resistance of implantation induced damage layers. We have used a vertical geometry test structure employed by previous workers<sup>(1,2,3,5,6)</sup> and a device-related lateral geometry test structure. In addition to the resistance of the as-implanted layers, the thermal stability of the damage layers was evaluated by measuring the layer resistance after a series of isochronal anneals.

Manuscript approved October 26, 1982.

## EXPERIMENTAL PROCEDURE

The geometries used for this work are shown in the first two figures. Figure 1 shows the vertical geometry. The backside was metallized with a AuGe/Au ohmic contact and the front surface contacted by a thin (compared to the maximum range of the incident particles) 12 mil diameter,  $1000\text{\AA}$  thick Au dot. The bulk samples used for the vertical geometry studies were  $3 \times 10^{16}/\text{cm}^3$ , (100), Sn-doped, n-type InP. A thin damage layer was produced under the front surface metallization with the ion of interest. The resistance of this layer was determined by measuring the current flow from the front to the back of the sample as a function of applied voltage. The as-deposited Au dot is rectifying but is rendered ohmic by the particle irradiation. Since the bulk InP has a much lower resistance than the damage layer, the resistance measured is that of the damage layer.

The lateral geometry, employed to reflect the structures of technological interest, is shown in Figure 2. In this configuration, a damage region defined by thick (compared to the maximum range of the incident particles), concentric, circular metallizations, was implanted. The resistance of this layer was determined by measuring the current flow between the concentric metallizations as a function of applied voltage. For this part of the study,  $10^{17} \text{ cm}^{-3}$ , n-type, vapor-phase-epitaxial (VPE) layers grown on Fe-doped semi-insulating InP substrates were used. The metallizations were 3  $\mu\text{m}$  thick Au, plated onto AuGe/Au ohmic contacts to the surface.

Damage layers produced by the multiple energy implantation of H, He, Be, and B were investigated with each geometry. The implant schedule for the vertical structure was designed to produce the thickest layers possible with the energies available. The schedules selected for the lateral structures were designed to penetrate the VPE layer. The details of the implant schedules are

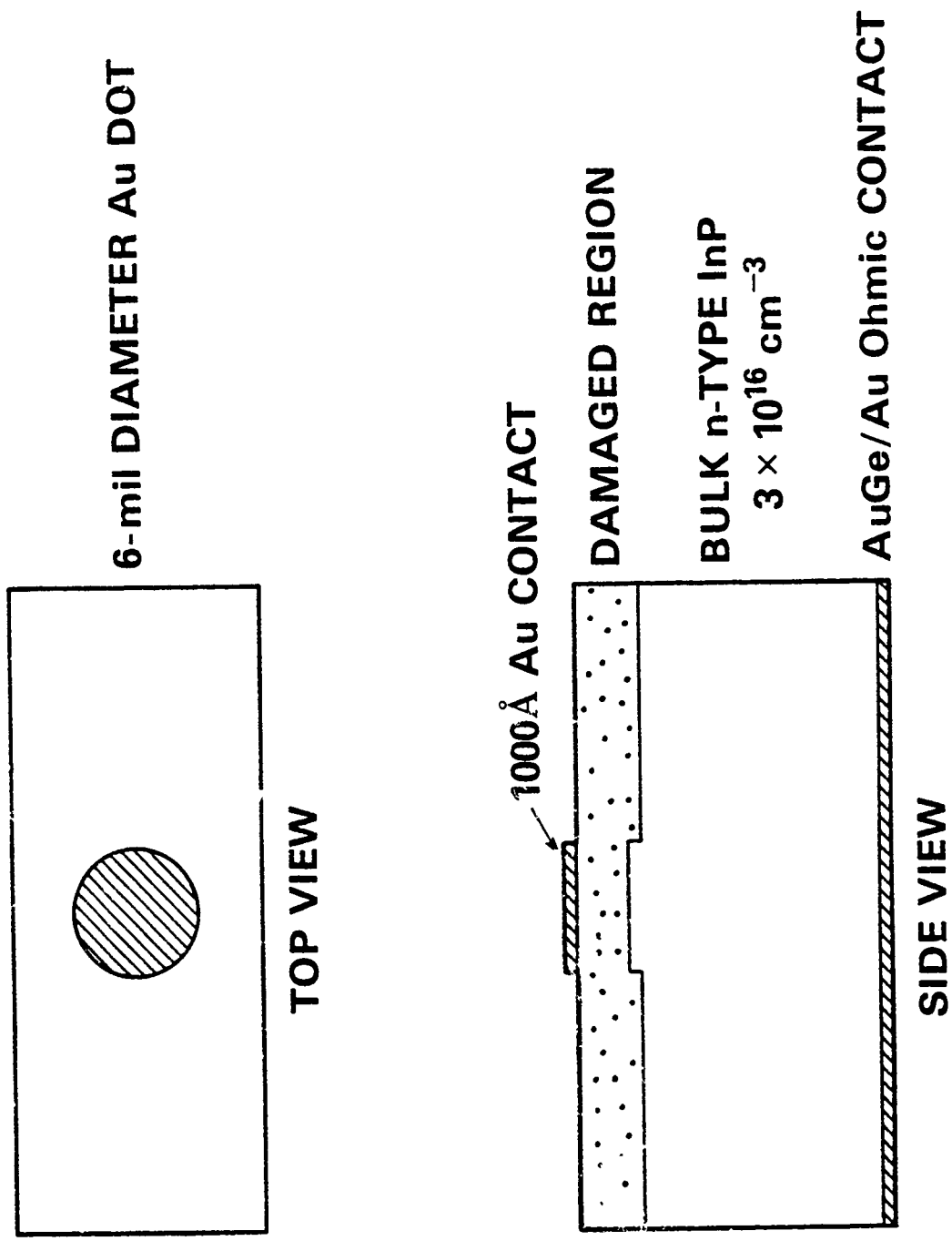
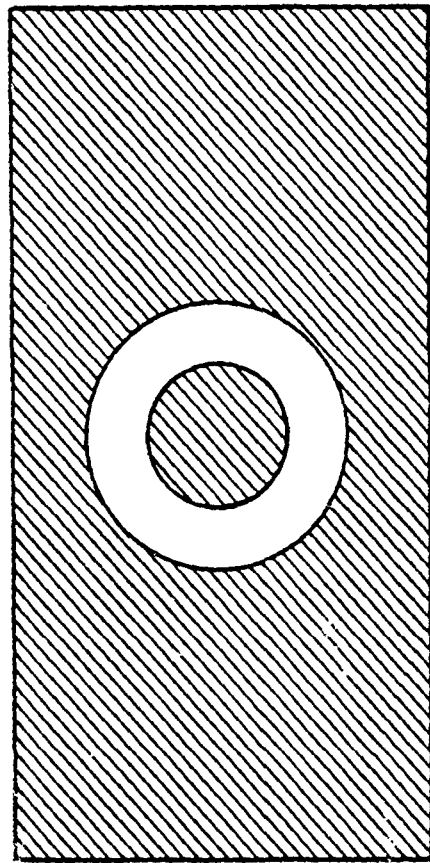
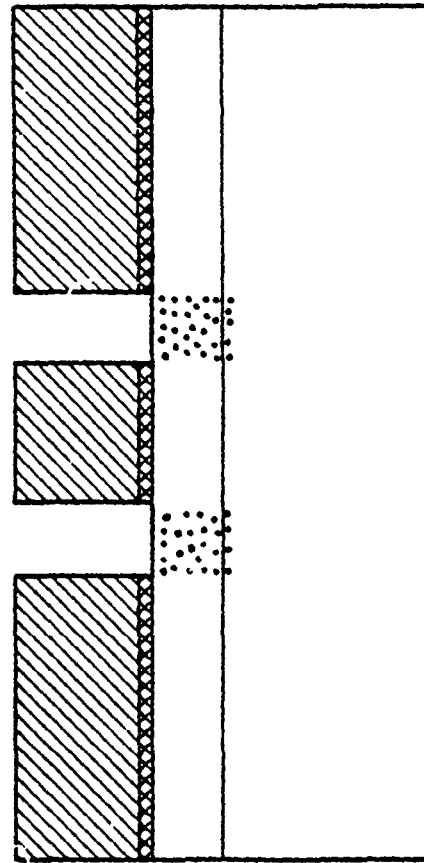


Figure 1. The vertical geometry test structure fabricated on bulk n-type InP,  $3 \times 10^{16} / \text{cm}^3$ .



**TOP VIEW**



**SIDE VIEW**

3 μm PLATED Au  
 AuGe/Au Ohmic CONTACT  
 0.5 μm EPITAXIAL LAYER  
 n-TYPE  $1 \times 10^{17} \text{ cm}^{-3}$   
 Fe-DOPED  
 SI-SUBSTRATE

Figure 2. The lateral geometry test structure fabricated on epitaxial n-type InP,  $1 \times 10^{17} / \text{cm}^3$ , on a Fe-doped InP SI substrate.

given in Tables 1 and 2. The calculated projected ranges cited for the vertical geometry have been corrected for the energy loss in the Au contact.<sup>(4)</sup>

To facilitate the comparison of a variety of experiments, it is useful to express the results in terms of resistivities. For the vertical structure, the resistivity of the damage layer was calculated from

$$\rho = RA/L$$

where A = Area of Au dot

L = Depth of damage

For the lateral structure, the resistivity was calculated from

$$\rho = 2\pi RT \left[ \ln \left[ \frac{R_A + R_B}{R_A} \right] \right]^{-1}$$

where T = Thickness of VPE layer (0.5  $\mu\text{m}$ )

$R_A$  = Radius of center (58  $\mu\text{m}$ )

$R_B$  = Radius of perimeter (110  $\mu\text{m}$ )

## RESULTS

### A) Vertical Isolation

The resistivity of the damaged layer as a function of implant dose is shown for each ion in Figure 3. For all the ions, there is an optimum dose for maximum isolation. At lower doses, the resistivity increases with dose. In this regime, more defects are being formed to trap carriers and reduce the mobility of the remaining electrons. At higher doses, the resistivity decreases with dose. Two mechanisms have been suggested to explain this; the banding of defect levels,<sup>(2)</sup> and the onset of hopping conduction.<sup>(6)</sup> The maximum resistivity observed for each ion is between  $10^3$  and  $10^4$  ohm $\cdot$ cm. The highest resistivity ( $7 \times 10^3$  ohm $\cdot$ cm) was observed with He bombardment. The implant concentration corresponding to the maximum in the resistivity versus dose curve

TABLE 1 - IMPLANT SCHEDULE

VERTICAL TEST STRUCTURE

ION	ENERGY-RELATIVE FLUENCE	FLUENCE $\text{cm}^{-2}$	DOSE $\text{cm}^{-3}$	PROJECTED RANGE OF IMPLANT
H	300 keV - N	$N = 10^{13}$	$1.5 \times 10^{17}$	2.6 $\mu\text{m}$
	240 keV - 0.8N	$N = 10^{14}$	$1.5 \times 10^{18}$	
	180 keV - 0.7N	$N = 5 \times 10^{14}$	$7.5 \times 10^{18}$	
	125 keV - 0.65N	$N = 10^{15}$	$1.5 \times 10^{18}$	
	75 keV - 0.55N	$N = 10^{16}$	$1.5 \times 10^{20}$	
	40 keV - 0.44N			
	13 keV - 0.25N			
He	300 keV - N	$N = 10^{12}$	$1.85 \times 10^{16}$	1.2 $\mu\text{m}$
	190 keV - 0.7N	$N = 10^{13}$	$1.85 \times 10^{17}$	
	100 keV - 0.47N	$N = 10^{14}$	$1.85 \times 10^{18}$	
	50 keV - 0.285N			
	20 keV - 0.176N			
Be	550 keV - N	$N = 10^{11}$	$1.6 \times 10^{15}$	1.5 $\mu\text{m}$
	340 keV - 0.63N	$N = 10^{12}$	$1.6 \times 10^{16}$	
	170 keV - 0.53N	$N = 10^{13}$	$1.6 \times 10^{17}$	
	80 keV - 0.24N	$N = 10^{14}$	$1.6 \times 10^{18}$	
	40 keV - 0.17N	$N = 3 \times 10^{14}$	$4.8 \times 10^{18}$	
B	300 keV - N	$N = 10^{12}$	$1.75 \times 10^{16}$	0.8 $\mu\text{m}$
	170 keV - 0.53N	$N = 10^{13}$	$1.75 \times 10^{17}$	
		$N = 5 \times 10^{13}$	$8.75 \times 10^{17}$	

TABLE 2 - IMPLANT SCHEDULE

LATERAL TEST STRUCTURE

ION	ENERGY-RELATIVE FLUENCE	FLUENCE cm <sup>-2</sup>	DOSE cm <sup>-3</sup>	PROJECTED RANGE OF IMPLANT
H	80 keV - N 40 keV - 0.65N 13 keV - 0.41N	N = 4.22x10 <sup>11</sup>	10 <sup>16</sup>	0.8 μm
		N = 4.22x10 <sup>12</sup>	10 <sup>17</sup>	
		N = 4.22x10 <sup>13</sup>	10 <sup>18</sup>	
		N = 1.27x10 <sup>14</sup>	3x10 <sup>18</sup>	
		N = 4.22x10 <sup>14</sup>	10 <sup>19</sup>	
He	160 keV - N 90 keV - 0.6N 40 keV - 0.48N 15 keV - 0.22N	N = 8.4x10 <sup>12</sup>	2x10 <sup>17</sup>	0.8 μm
Be	300 keV - N 160 keV - 0.52N 60 keV - 0.33N 20 keV - 0.11N	N = 6.4x10 <sup>12</sup>	9x10 <sup>16</sup>	0.9 μm
B	300 keV - N 160 keV - 0.52N 60 keV - 0.33N 20 keV - 0.11N	N = 6.4x10 <sup>9</sup>	10 <sup>14</sup>	0.8 μm
		N = 6.4x10 <sup>10</sup>	10 <sup>15</sup>	
		N = 6.4x10 <sup>11</sup>	10 <sup>16</sup>	
		N = 6.4x10 <sup>12</sup>	10 <sup>17</sup>	
		N = 6.4x10 <sup>13</sup>	10 <sup>18</sup>	

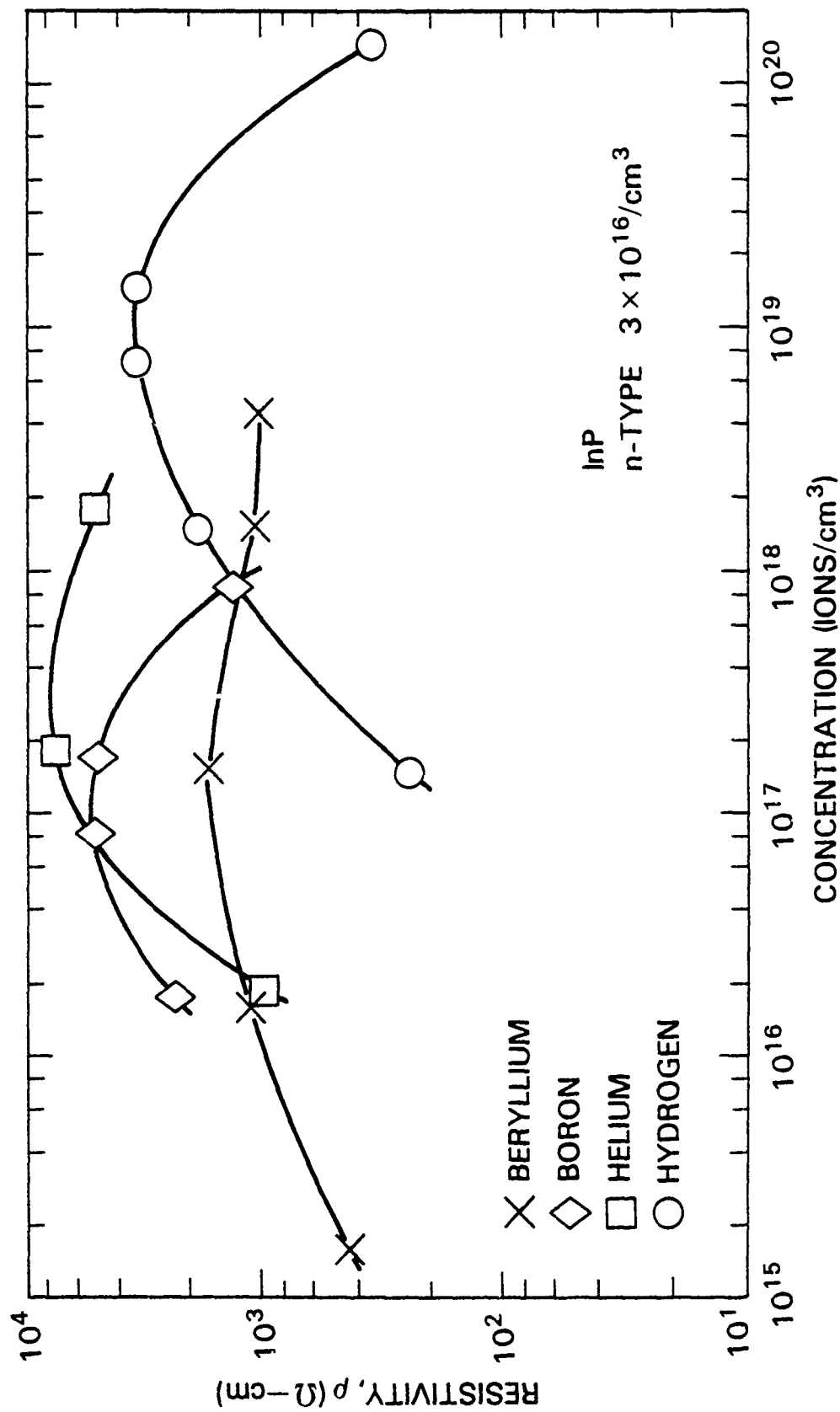


Figure 3. Average resistivity of the as-implanted region as a function of implantation concentration. The low voltage I-V characteristics were measured using the vertical test structure on bulk n-type InP,  $3 \times 10^{16}/\text{cm}^3$ .

is  $2 \times 10^{17}$ ,  $1.5 \times 10^{17}$  and  $1.6 \times 10^{17}$   $\text{cm}^{-3}$  for He, Be, and B, respectively. However, for H the maximum occurs at  $7.5 \times 10^{18}$   $\text{cm}^{-3}$ . These results are summarized in Table 3. The results of this portion of the work coincide with the previous work of Donnelly and Hurwitz.<sup>(2)</sup> These workers obtained a resistivity of 3 to  $4 \times 10^3$  ohm·cm with multiple energy proton implantation.

#### B) Lateral Structure

The boron implantation results obtained with the lateral test structure are shown in Figure 4. As with the vertical geometry test structure, there is a relative maximum in the resistivity at  $10^{17}$  B/cm<sup>3</sup>. The maximum resistivity is  $1.5 \times 10^3$  ohm·cm. Therefore, for boron implantation, there is good agreement between the vertical and lateral test structure results. However, for proton implantation, there is striking disagreement between the isolation achieved with the vertical and lateral test structures. For the lateral test structure the maximum resistivity obtained with the proton implantation was 2 ohm·cm, (see Figure 5) compared to  $3 \times 10^3$  ohm·cm obtained using the vertical test structure. He and Be implantation were also used with the lateral test structure. The maximum resistivities achieved with these ions were  $1.7 \times 10^3$  and  $1.8 \times 10^3$  ohm·cm, respectively. Again, these values are in good agreement with the results using the vertical test structure. Thus, for the light ions considered, the proton implantation was unique with respect to the poor isolation obtained with the lateral test structure. A summary of these results is given in Table 4.

#### C) Additional Studies of Proton Induced Damage

To obtain low resistivity (2 ohm·cm) in the lateral case and high resistivity ( $3 \times 10^3$  ohm·cm) in the vertical case implies that there is a low-resistivity layer in series with the measurement in the vertical case and in parallel to the measurement in the lateral case. The two most likely locations

TABLE 3

## MAXIMUM ISOLATION-VERTICAL TEST STRUCTURE

ION	DOSE	FLUENCE AT HIGHEST ENERGY	RESISTIVITY
H	$7.5 \times 10^{18} / \text{cm}^3$	$5 \times 10^{14} / \text{cm}^2$ @ 300 keV	$3 \times 10^3 \Omega\text{-cm}$
He	$2 \times 10^{17} / \text{cm}^3$	$10^{13} / \text{cm}^2$ @ 300 keV	$7.6 \times 10^3 \Omega\text{-cm}$
Be	$1.6 \times 10^{17} / \text{cm}^3$	$10^{13} / \text{cm}^2$ @ 550 keV	$2.3 \times 10^3 \Omega\text{-cm}$
B	$1.75 \times 10^{17} / \text{cm}^3$	$10^{13} / \text{cm}^2$ @ 300 keV	$5 \times 10^3 \Omega\text{-cm}$

TABLE 4

## MAXIMUM ISOLATION-LATERAL TEST STRUCTURE

ION	DOSE	FLUENCE AT HIGHEST ENERGY	RESISTIVITY
H	$7.5 \times 10^{18} / \text{CM}^3$	$4.2 \times 10^{14} / \text{CM}^2$ @ 80 KEV	$2.3 \Omega\text{-CM}$
HE	$2 \times 10^{17} / \text{CM}^3$	$8.4 \times 10^{12} / \text{CM}^2$ @ 160 KEV	$1.7 \times 10^3 \Omega\text{-CM}$
BE	$9 \times 10^{16} / \text{CM}^3$	$6.4 \times 10^{12} / \text{CM}^2$ @ 300 KEV	$1.8 \times 10^3 \Omega\text{-CM}$
B	$1 \times 10^{17} / \text{CM}^3$	$6.4 \times 10^{12} / \text{CM}^2$ @ 300 KEV	$1.5 \times 10^3 \Omega\text{-CM}$

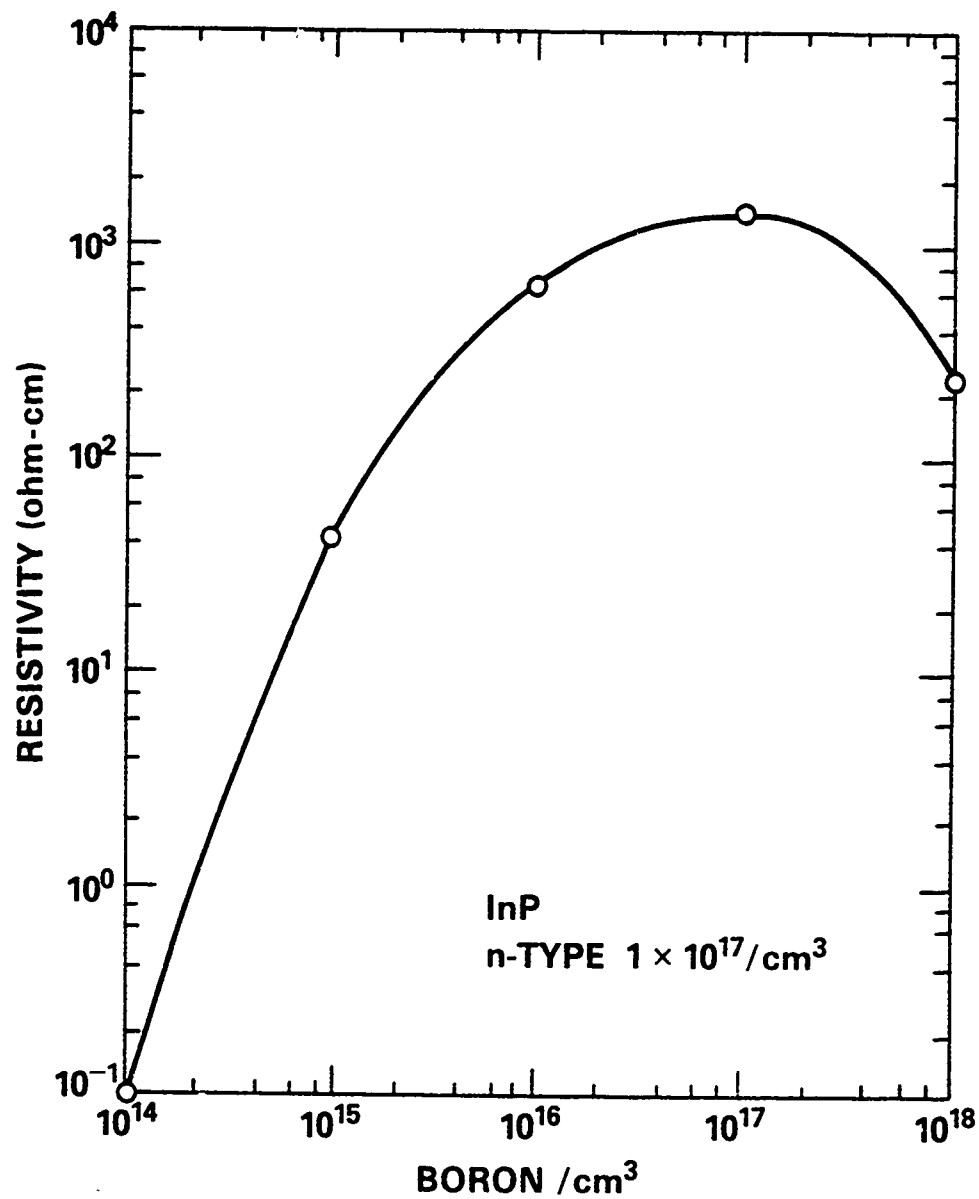


Figure 4. Average resistivity of the as-implanted region as a function of Boron concentration. The low voltage I-V characteristics were measured using the lateral test structure on epitaxial n-type InP,  $1 \times 10^{17}/\text{cm}^3$ .

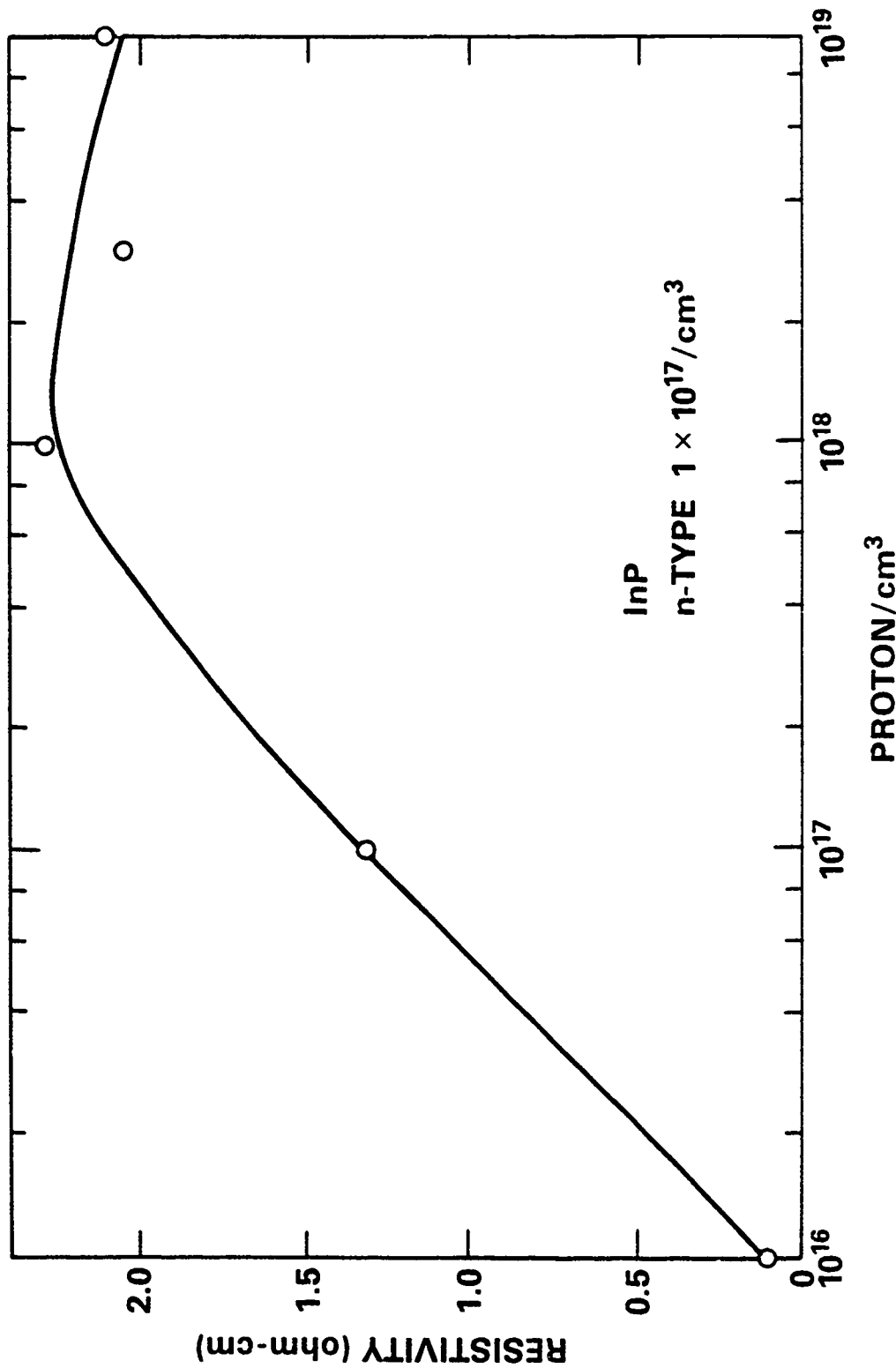


Figure 5. Average resistivity of the as-implanted region as a function of proton concentration. The low voltage I-V characteristics were measured using the lateral test structure on epitaxial n-type InP,  $1 \times 10^{17}/\text{cm}^3$ .

of such a shunting layer are the surface of the sample and the interface of the VPE layer and the SI substrate. To test the hypothesis of a surface low-resistivity layer, a sample already implanted with protons was further implanted with 15 keV He at a fluence of  $1.86 \times 10^{12} \text{ cm}^{-2}$ . The low energy He implant significantly damaged the surface, but there was no change in resistivity. For additional verification, an unimplanted lateral geometry sample was implanted with He at the front half of the VPE layer and H at the back half.

He	40 keV	$4 \times 10^{12} \text{ cm}^{-2}$
	15 keV	$1.68 \times 10^{12} \text{ cm}^{-2}$
H	80 keV	$4.22 \times 10^{14} \text{ cm}^{-2}$
	40 keV	$2.76 \times 10^{14} \text{ cm}^{-2}$

Again, the as-implanted resistivity was  $2 \text{ ohm}\cdot\text{cm}$ . Since it has already been shown that He at this fluence produces resistivity of  $2 \times 10^3 \text{ ohm}\cdot\text{cm}$ , the front of the sample is isolated. Apparently the low resistivity layer is near the VPE-substrate interface.

To check this hypothesis, three experiments were performed. The first was a continuation of the He-H implant study. The specimen implanted with 40 and 15 keV He and 80 and 40 keV H was further implanted sequentially with 90, 160, and 280 keV He. The resistivities obtained were  $2.9 \times 10^2$ ,  $7.8 \times 10^2$ , and  $9.8 \times 10^2 \text{ ohm}\cdot\text{cm}$ , respectively. It is seen that the 160 keV He, which has almost the same range as the 80 keV H, and the 280 keV He implants yield resistivities close to  $10^3 \text{ ohm}\cdot\text{cm}$ . Therefore, the shunting layer is not at the surface and is near the end of the implant range.

The second experiment was a study of isolation versus range of the protons. A low resistivity layer would be found near the VPE-substrate interface if the protons did not have enough energy to penetrate the VPE layer. In the

original implants, a maximum proton energy of 80 keV was chosen since the calculated projected range was 0.77  $\mu\text{m}$ , more than 150% of the 0.5  $\mu\text{m}$  VPE layer. A set of implants were performed at even higher energies to guarantee that the damage is well beyond the VPE-substrate interface. A sample which had been implanted with 80, 40, 13 keV protons was implanted, sequentially, with: 130 keV,  $3.25 \times 10^{14}$  H/cm<sup>2</sup>; 185 keV,  $3.5 \times 10^{14}$  H/cm<sup>2</sup>; 240 keV,  $4 \times 10^{14}$  H/cm<sup>2</sup>; and 300 keV,  $5 \times 10^{14}$  H/cm<sup>2</sup>. Only a minor increase in resistivity was seen. Since the calculated range of 300 keV protons in InP is 2.6  $\mu\text{m}$ , it is unlikely that the damage caused by these ions does not extend past the VPE layer.

The third experiment investigated the interaction of the protons with the SI substrate. The resistivity of the Fe-doped InP was measured as a function of proton dose. The specimen preparation was identical to the lateral test structure preparation, Figure 2, with the following exceptions: 1) Fe-doped SI InP was used instead of VPE n-type InP; and 2) prior to evaporation and plating of the Au on the front surface, Si was implanted and activated so that an active layer,  $n = 2 \times 10^{17}$  cm<sup>-3</sup>, having a thickness of 0.6  $\mu\text{m}$  was beneath the Au. During the Si implantation, the region between the concentric contacts was masked with 2  $\mu\text{m}$  of photoresist to maintain the SI property of this area. For the experiment, the sample was implanted with protons (80 keV, 40 keV, 13 keV). The low voltage I-V characteristics were measured as before. The resistivity of the SI InP as a function of proton concentration is shown in Figure 6. For doses equal to or less than  $5 \times 10^{15}$  H/cm<sup>2</sup>, the substrate remained SI, but for greater doses, the resistivity decreased monotonically with dose. Between  $10^{18}$  H/cm<sup>2</sup> and  $10^{19}$  H/cm<sup>2</sup>, where the isolation on the VPE sample was a maximum, the substrate had a resistivity between 60 ohm $\cdot$ cm and 20 ohm $\cdot$ cm. Apparently, the activation of the SI substrate is a significant factor in the low resistivities measured on the proton implanted lateral test structures.

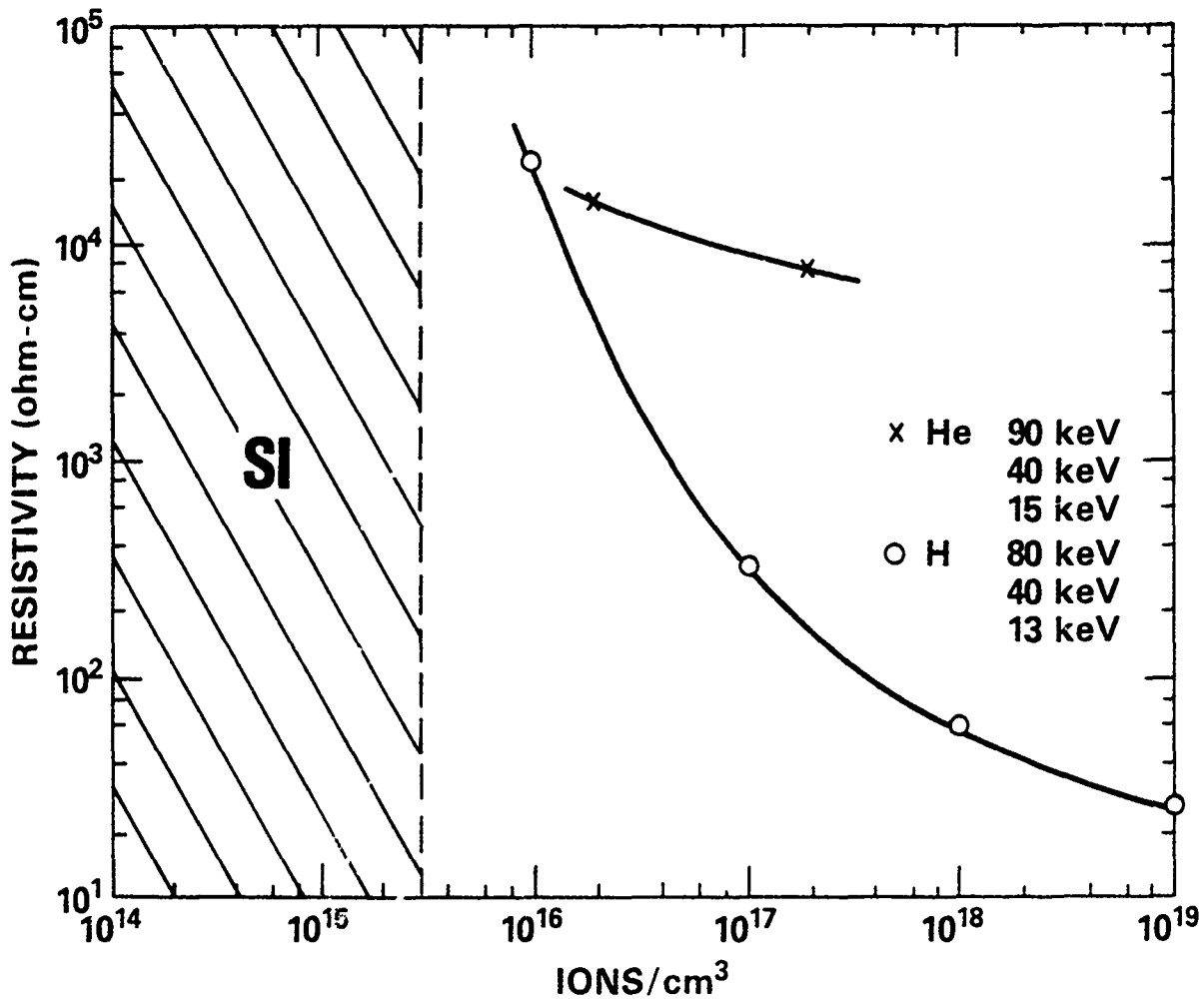


Figure 6. The variation of the average resistivity of Fe-doped InP as a function of H and He implant concentration. The low voltage I-V characteristics were measured using the lateral test structure.

Activation of the Fe-doped SI substrate was also measured for He implantation. Resistivity as a function of dose is shown in Figure 6. The He implant also decreased the resistivity of the Fe-doped InP but to a lesser degree than the protons. The optimum dose for resistivity using He implantation is  $10^{17} \text{ cm}^{-3}$ . The resistivity of the n-type InP implanted at this dose with He is  $10^3 \text{ ohm}\cdot\text{cm}$ , which is less than the  $10^4 \text{ ohm}\cdot\text{cm}$  measured in the Fe-doped InP at the same He dose. Therefore, the slight activation seen with He implantation in Fe-doped InP would not affect the lateral resistivity values.

#### D) Anneal Study

The thermal stability of the damage layers was investigated using samples prepared with the vertical test structure. 30 minute isochronal anneals were carried out in  $50^\circ\text{C}$  steps. The low voltage I-V characteristics were measured between each step. The effect of temperature on the resistivity as a function of dose for each ion is presented in Figures 7-10.

For the H implant, Figure 7, the low dose implant ( $1.5 \times 10^{17} \text{ H/cm}^3$ ) has an anneal stage between  $50^\circ\text{C}$  and  $100^\circ\text{C}$ . All the higher dose implants maintain a resistivity greater than  $10^3 \text{ ohm}\cdot\text{cm}$  up to  $250^\circ\text{C}$ . Then there is a rapid anneal stage which reduces the resistivity to  $\sim 10 \text{ ohm}\cdot\text{cm}$ . At this stage, the low voltage I-V characteristics are no longer linear but are those of leaky Schottky barriers.

The He implant, Figure 8, has similar anneal properties. The low dose implant ( $1.85 \times 10^{16} \text{ He/cm}^3$ ) has an anneal stage between  $50^\circ\text{C}$  and  $100^\circ\text{C}$ . The optimum dose implant ( $1.85 \times 10^{17} \text{ He/cm}^3$ ) maintains its resistivity above  $2 \times 10^3 \text{ ohm}\cdot\text{cm}$  to  $300^\circ\text{C}$ . The highest dose implant is least affected by temperature. In fact, there is an increase in the resistivity between  $300^\circ\text{C}$  and  $400^\circ\text{C}$ . The results of the anneal studies of the Be and B implanted samples demonstrate similar characteristics, Figures 9 and 10.

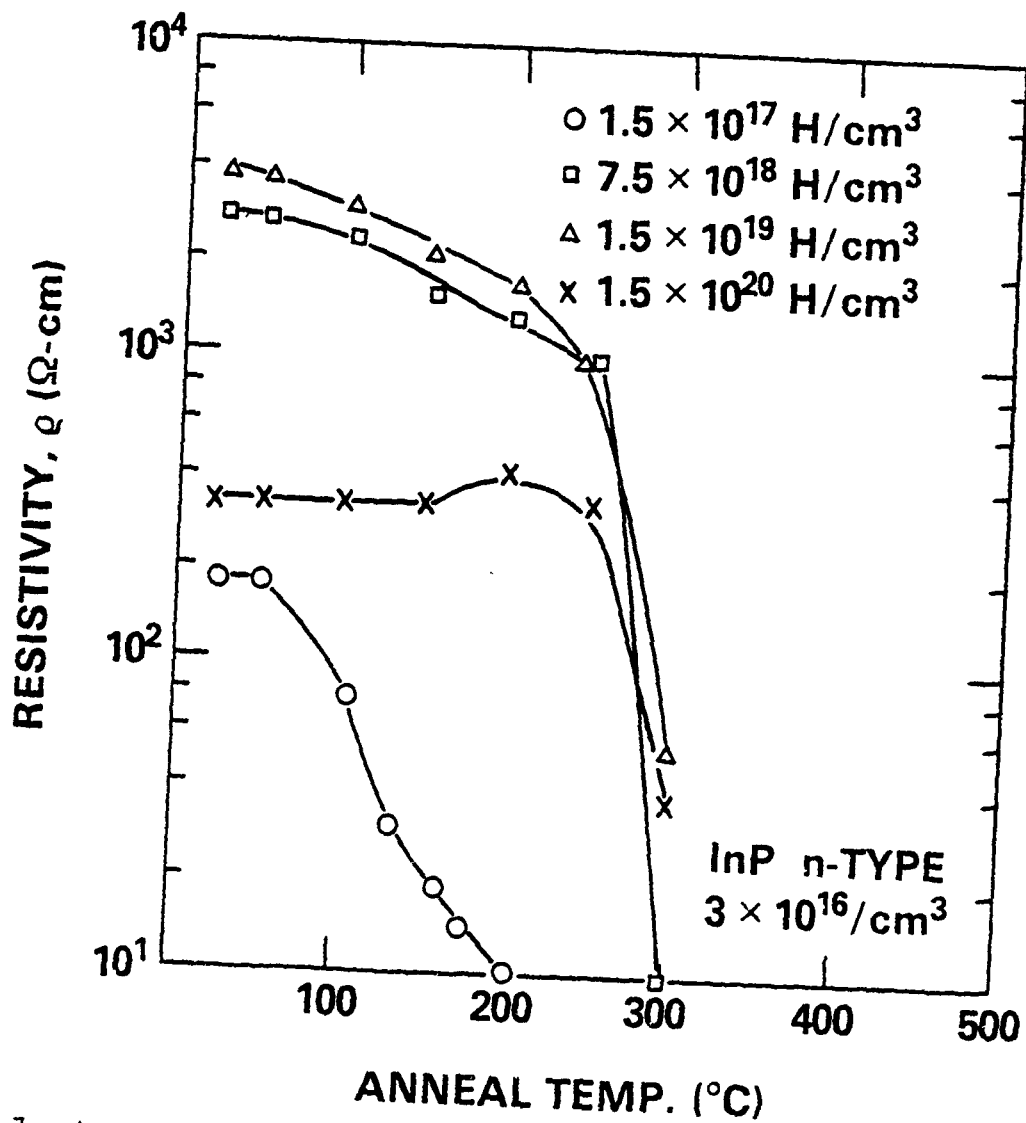


Figure 7. Anneal characteristics of Hydrogen implanted InP. 30 minute, isochronal anneal at 50 $^{\circ}$ C steps were performed in flowing forming gas. The low voltage I-V characteristics were measured using the vertical test structure on n-type InP,  $3 \times 10^{16}$ /cm<sup>3</sup>.

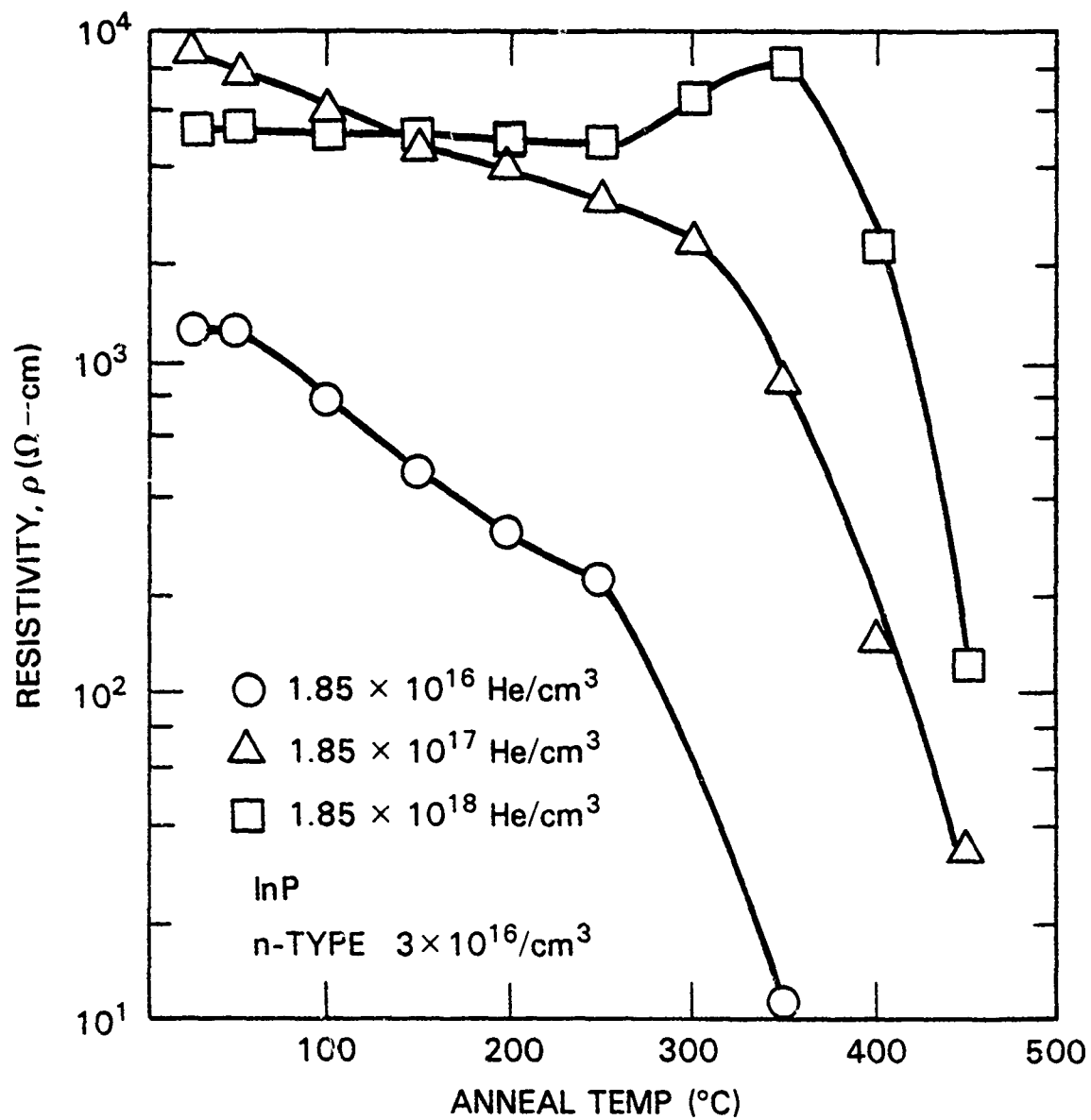


Figure 8. Anneal characteristics of Helium implanted InP. 30 minute isochronal anneal at 50 $^{\circ}$ C steps were performed in flowing forming gas. The low voltage I-V characteristics were measured using the vertical test structure on n-type InP,  $3 \times 10^{16}$ /cm<sup>3</sup>.

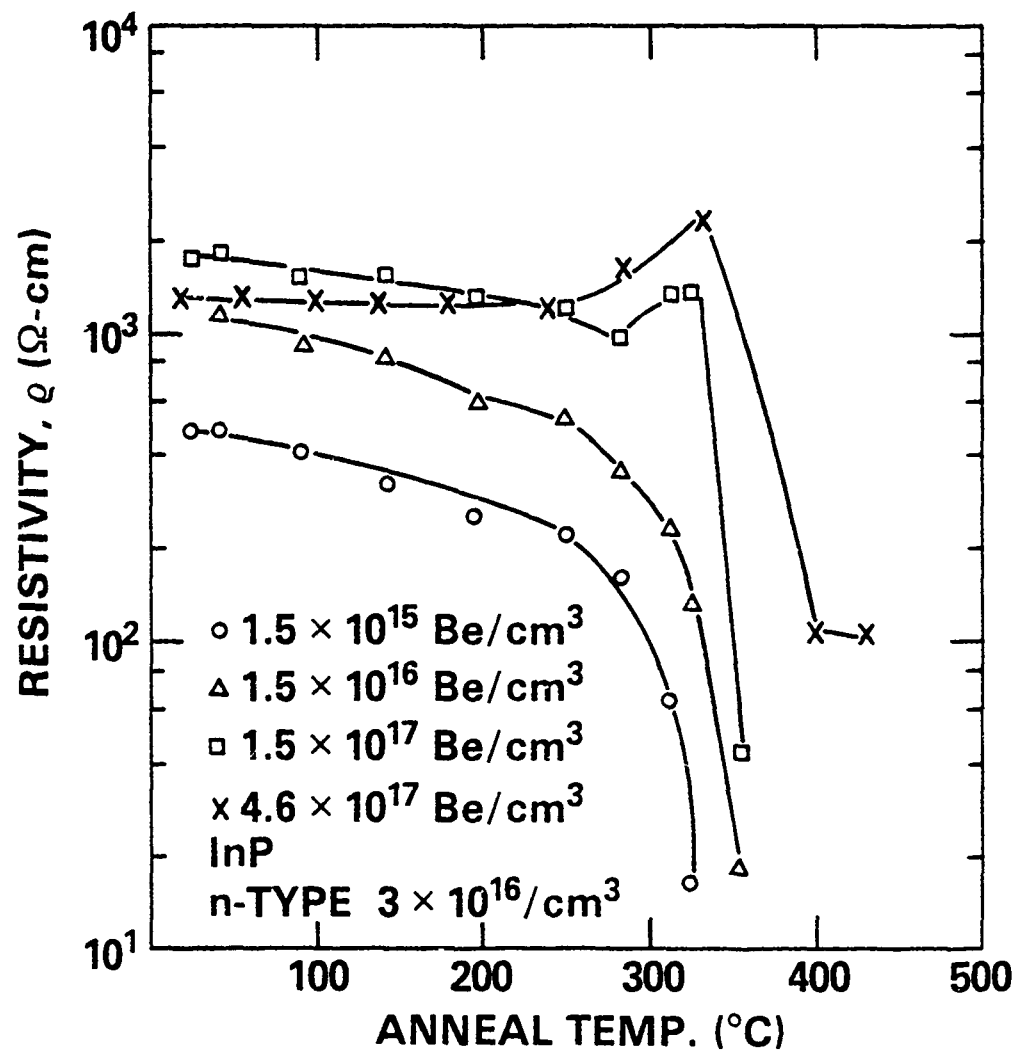


Figure 9. Anneal characteristics of Beryllium implanted InP. 30 minute, isochronal anneal at  $50^{\circ}$ C steps were performed in flowing forming gas. The low voltage I-V characteristics were measured using the vertical test structure on n-type InP,  $3 \times 10^{16}$ /cm<sup>3</sup>.

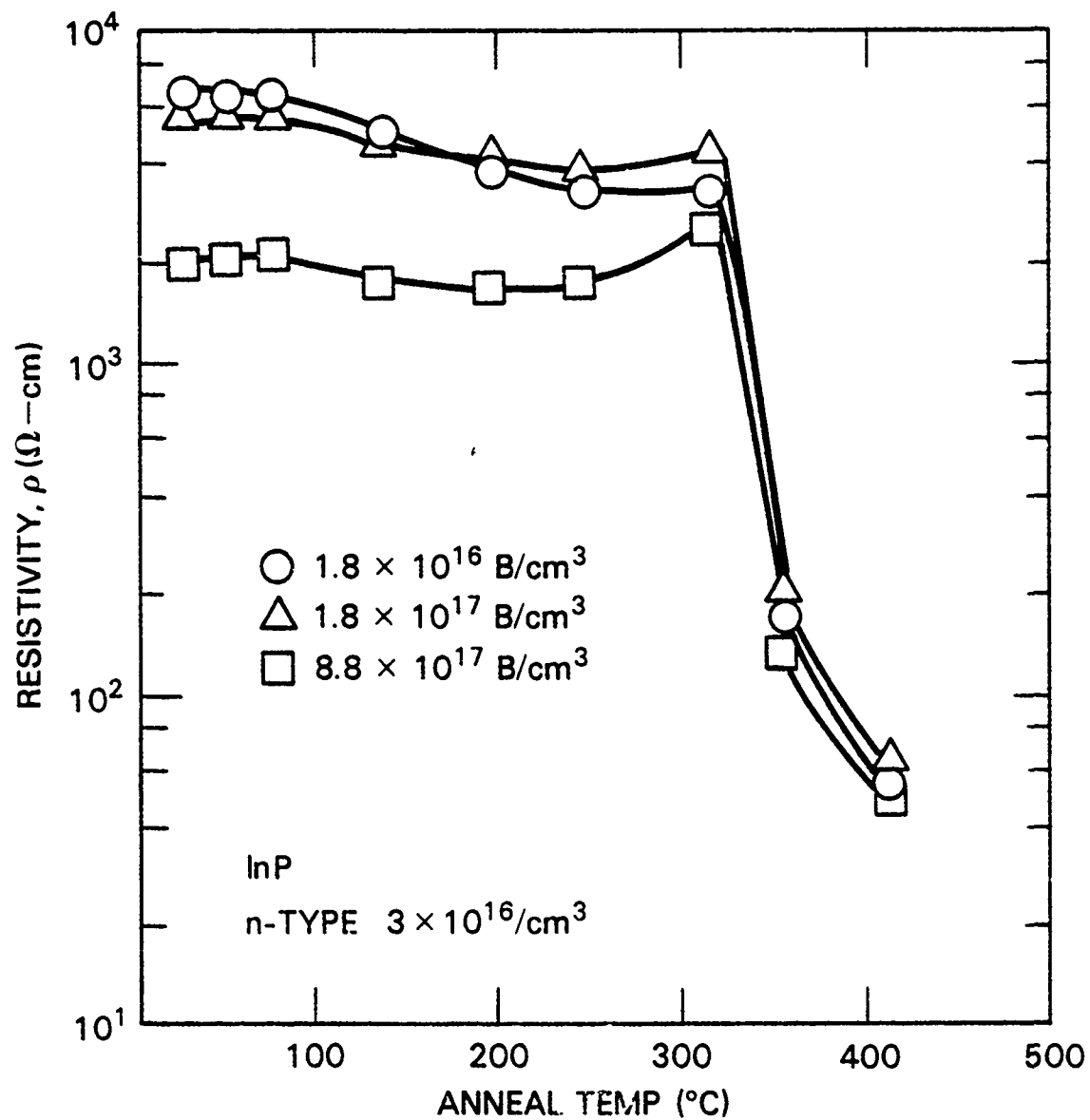


Figure 10. Anneal characteristics of Boron implanted InP. 30 minute isochronal anneal at 50 $^{\circ}$ C steps were performed in flowing forming gas. The low voltage I-V characteristics were measured using the vertical test structure on n-type InP,  $3 \times 10^{16}$ /cm<sup>3</sup>.

## CONCLUSION

A detailed study of damage induced isolation in n-type InP by light ion implantation has been completed. Two test structures have been utilized, a vertical test structure and a lateral test structure. The thermal stability of the damage layers were also investigated.

Using the vertical geometry test structure, resistivity versus dose curves were measured for H, He, Be, and B implantation. For each ion there was an optimum dose for maximum resistivity;  $7.5 \times 10^{18}$  H/cm<sup>3</sup>,  $2 \times 10^{17}$  He/cm<sup>3</sup>,  $1.6 \times 10^{17}$  Be/cm<sup>3</sup>, and  $1.75 \times 10^{17}$  B/cm<sup>3</sup>. Resistivities of  $10^3$  to  $10^4$  ohm·cm were obtained with these ions. The maximum resistivity observed was  $7.6 \times 10^3$  ohm·cm. This was obtained with He implantation. With the same geometry, Donnelly and Hurwitz<sup>(2)</sup> obtained a resistivity of 3 to  $4 \times 10^3$  ohm·cm with multiple energy proton implantation.

The results using the lateral geometry test structure corresponded well to those using the vertical test structure for He, Be, and B implantation but not H implantation. The maximum resistivity obtained with the H implantation was only 2 ohm·cm. It has been demonstrated that one of the causes of this disparity is the reduction in the resistivity of the Fe-doped InP substrate due to proton implantation. This low resistivity layer, acting as a shunt, dominates the lateral geometry test structure I-V measurements. The He implantation also reduced the resistivity of the Fe-doped substrate, but the reduction was not sufficient to affect the lateral geometry test structure I-V measurements.

The damage induced dielectric isolation has been shown to be thermally stable up to 250°C for H and greater than 300°C for He, Be, and B for the doses producing maximum resistivity. At low dose, there is an anneal stage which begins between 50°C and 100°C. Therefore, there must be qualitatively

at least two forms of defects affecting the isolation. Likely candidates are isolated point defects for the low dose case and aggregates of these defects in the high dose case.

In conclusion, it has been shown that proton bombardment is unsuitable for the lateral isolation of epitaxial structures on Fe-doped SI InP. A conductive layer is produced by the protons which enter the SI substrate and this results in a low-resistance shunt in parallel with the interdevice isolation. He, Be or B implantation at doses of  $2 \times 10^{17} \text{ cm}^{-3}$  produces damage layers which have a resistivity of  $10^3$ - $10^4 \text{ ohm}\cdot\text{cm}$ . These layers are thermally stable to anneal temperatures of  $300^\circ\text{C}$  and can be used to isolate bulk n-type material or n-type epitaxial layers which have been grown on Fe-doped substrates.

#### REFERENCES

1. J. P. Donnelly and F. J. Lenberger, *Solid State Electronics*, 20, 183 (1977).
2. J. P. Donnelly and C. E. Hurwitz, *Solid State Electronics*, 20, 727 (1977).
3. J. P. Donnelly and C. E. Hurwitz, *Solid State Electronics* 21, 475 (1978).
4. J. F. Gibbons, W. S. Johnson, and S. W. Mylroie, Projected Range Statistics, 2nd Ed., Dowden, Hutchinson, and Ross, Inc., Stroudsburg, Pa., 1975.
5. J. C. Dymant, J. C. North, and L. A. D'Asaro, *J. Appl. Phys.*, 44, 207, (1973).
6. K. Steeples, I. J. Saunders, and J. G. Smith, *IEEE Electron Device Letters*, EDL-1, No. 5, 72 (1980).